HUMAN GENE THERAPY 21:451–462 (April 2010)

DOI: 10.1089/hum.2009.111

Safety Studies on Intrahepatic or Intratumoral Injection of Oncolytic Vesicular Stomatitis Virus Expressing Interferon-β in Rodents and Nonhuman Primates

Nathan Jenks,[1,2] Rae Myers,[1,2] Suzanne M. Greiner,[1,2] Jill Thompson,[2] Emily K. Mader,[2] Andrew Greenslade,[1,2] Guy E. Griesmann,[2,3] Mark J. Federspiel,[2,3] Jorge Rakela,[4] Mitesh J. Borad,[4] Richard G. Vile,[2] Glen N. Barber,[5] Thomas R. Meier,[6] Michael C. Blanco,[6] Stephanie K. Carlson,[2,7] Stephen J. Russell,[2] and Kah-Whye Peng[1,2]

Abstract

Toxicology studies were performed in rats and rhesus macaques to establish a safe starting dose for intratumoral injection of an oncolytic vesicular stomatitis virus expressing human interferon-β (VSV-hIFNβ) in patients with hepatocellular carcinoma (HCC). No adverse events were observed after administration of 7.59×10^9 $TCID_{50}$ (50% tissue culture infective dose) of VSV-hIFNβ into the left lateral hepatic lobe of Harlan Sprague Dawley rats. Plasma alanine aminotransferase and alkaline phosphatase levels increased and platelet counts decreased in the virus-treated animals on days 1 and 2 but returned to pretreatment levels by day 4. VSV-hIFNβ was also injected into normal livers or an intrahepatic McA-RH7777 HCC xenograft established in Buffalo rats. Buffalo rats were more sensitive to neurotoxic effects of VSV; the no observable adverse event level (NOAEL) of VSV-hIFNβ in Buffalo rats was 10^7 $TCID_{50}$. Higher doses were associated with fatal neurotoxicity and infectious virus was recovered from tumor and brain. Compared with VSV-hIFNβ, toxicity of VSV-rIFNβ (recombinant VSV expressing rat IFN-β) was greatly diminished in Buffalo rats (NOAEL, $>10^{10}$ $TCID_{50}$). Two groups of two adult male rhesus macaques received 10^9 or 10^{10} $TCID_{50}$ of VSV-hIFNβ injected directly into the left hepatic lobe under computed tomographic guidance. No neurological signs were observed at any time point. No abnormalities (hematology, clinical chemistry, body weights, behavior) were seen and all macaques developed neutralizing anti-VSV antibodies. Plasma interleukin-6, tumor necrosis factor-α, and hIFN-β remained below detection levels by ELISA. On the basis of these studies, we will be proposing a cautious approach to dose escalation in a phase I clinical trial among patients with HCC.

Introduction

Approximately half a million people worldwide are diagnosed each year with hepatocellular carcinoma (HCC) and an equivalent number of patients die annually from this disease, making HCC the fifth most frequent cancer in the world and the third most common cause of cancer-related deaths (Parkin *et al.*, 2005). Risk factors for HCC include hepatitis B and C infections and alcoholism (Blum, 2005). Radical treatments include surgical resection, locoregional ablative techniques (radiofrequency ablation, transarterial chemoembolization, or percutaneous ethanol injection), and liver transplantation or partial hepatectomy, but recurrence rates remain as high as 60% (Kamiyama *et al.*, 2009; Verslype *et al.*, 2009). Factors that determine resectability include the degree of portal hypertension, bilirubin level, tumor size, multiple or bilobar lesions, vascular invasion, and extrahepatic spread. Present therapies for patients with unresectable HCC are limited in a small subset of patients to liver transplantation. Median survival of untreated patients in Western countries is

[1]Toxicology and Pharmacology Laboratory, Mayo Clinic, Rochester, MN 55905.
[2]Department of Molecular Medicine, Mayo Clinic, Rochester, MN 55905.
[3]Viral Vector Production Laboratory, Mayo Clinic, Rochester, MN 55905.
[4]Department of Internal Medicine, Transplantation Medicine, Mayo Clinic, Scottsdale, AZ 85259.
[5]Department of Medicine, University of Miami, Miami, FL 33136.
[6]Department of Comparative Medicine, Mayo Clinic, Rochester, MN 55905.
[7]Department of Radiology, Mayo Clinic, Rochester, MN 55905.

approximately 4 months. Even with "active" cytotoxic agents, such as doxorubicin and cisplatin, response rates are typically less than 10% (Verslype *et al.*, 2009). Median survival is 3 to 6 months and 5-year survival is less than 5% with these cytotoxic agents. Sorafenib has become the standard of care for advanced HCC; median survival of patients treated with sorafenib was 10.7 months compared with 7.9 months for the placebo arm (Llovet *et al.*, 2008). Given the limited treatment options for advanced HCC, there is an urgent need for novel therapeutics with alternative mechanisms of action, including the use of tumor-selective replicating viruses.

Numerous viruses from diverse families are being investigated as oncolytic agents (Russell and Peng, 2007). The Indiana strain of vesicular stomatitis virus (VSV) and its recombinant derivatives have promising oncolytic activity against a variety of tumor types (Barber, 2004; Lichty *et al.*, 2004). Vesicular stomatitis virus has a rapid life cycle; cytopathic effects (CPEs) are typically evident by 24 hr postinfection as virus-infected cells round up and die by apoptosis (Kopecky *et al.*, 2001). The burst size of a VSV-infected cell ranges between 500 and 6000 viruses per cell (Novella *et al.*, 2004). The virus is sensitive to the antiviral effects of interferon (IFN)-α/β produced by infected cells to limit viral replication and spread to neighboring cells. As such, the oncolytic VSVs in development for cancer therapy are modified to induce or produce high levels of type I interferon as a means to protect normal cells from cytolytic damage by the virus. For example, Bell and colleagues demonstrated that VSV with a mutation in amino acid 51 of the matrix (M) gene induced higher levels of type I IFN in normal cells and has a significantly higher 50% lethal dose (LD_{50}) after intranasal inoculation into mice compared with wild-type VSV (Stojdl *et al.*, 2003). Similarly, VSV expressing murine IFN-β (VSV-mIFNβ) or human IFN-β (VSV-hIFNβ) is nonlytic in normal cells and is less toxic than the wild-type virus *in vivo* (Obuchi *et al.*, 2003). Whereas the LD_{50} of wild-type VSV after intravenous administration into BALB/c mice was 5×10^6 plaque-forming units (PFU), the LD_{50} of VSV-mIFNβ was 1×10^8 PFU (Obuchi *et al.*, 2003). These IFN-inducing viruses retained their oncolytic activity against tumor cells *in vitro* and against tumor xenografts in mice (Ebert *et al.*, 2003; Obuchi *et al.*, 2003; Kottke *et al.*, 2008). A phase I–II dose escalation clinical trial has been proposed to test single-dose direct intratumoral injection of VSV-hIFNβ into a discrete HCC nodule under ultrasound guidance at the Mayo Clinic in Scottsdale, Arizona (principal investigator, Mitesh Borad). The patients will be closely monitored in the hospital after virus administration and a variety of tissue samples will be harvested for correlative studies to determine the extent of viral replication and antitumor and antiviral immune responses. As such, preclinical toxicology and pharmacology studies were performed to test the safety of this therapeutic strategy and to establish a safe starting dose for the proposed clinical trial.

There are unique considerations regarding choice of an animal model for toxicology studies of virotherapy agents. Importantly, the host animal should be permissive to viral replication and the transgene should be biologically active in the chosen species. For this study, pharmacology/toxicology personnel in the Office of Cellular, Tissue, and Gene Therapies (OCTGT) in the Center for Biologics Evaluation and Research (CBER) of the U.S. Food and Drug Administration (FDA) had recommended that toxicology studies should include direct injection of the test article into an orthotopic HCC tumor in rats to model the clinical scenario. Ebert and colleagues previously established a syngeneic rat McA-RH7777 HCC model, in which discrete tumor xenografts can be surgically implanted in the hepatic lobes of Buffalo rats, and demonstrated that these tumor xenografts were susceptible to the oncolytic effects of VSV (Ebert *et al.*, 2003). A limitation with this tumor model is that only short-term toxicity studies can be performed as the tumors are aggressive in growth and the animals typically exhibit high plasma alanine aminotransferase (ALT) levels and succumb to tumor burden within the first 3 weeks. Hence, additional toxicity studies involving interim (day 44) and long-term (day 91) toxicity were also performed by direct intrahepatic injection of the test article into the liver of tumor-free rats (see Fig. 1). Because the test article (VSV-hIFNβ) expresses the human IFN-β protein, which is not biologically active in rodents, a recombinant VSV expressing a species-specific rat IFN-β was constructed in the laboratory of G. Barber (University of Miami, Miami, FL). The VSV-hIFNβ and VSV-rIFNβ viruses used in this study were manufactured according to a production strategy similar to that used by the Mayo Clinic Molecular Medicine Viral Vector Production Facility for the production of cGMP clinical lots. Because wild-type VSV causes serious clinical symptoms (fatal neurotoxicity) in rodents and nonhuman primates (Johnson *et al.*, 2007), we have also tested the safety of recombinant VSV-hIFNβ in rhesus macaques after intrahepatic injection under computed tomography (CT) guidance. Here, we report on the toxicology findings after intrahepatic or intratumoral injection of VSV-hIFNβ or VSV-rIFNβ into rats and nonhuman primates.

Materials and Methods

Tissue culture

The rat HCC cell line McA-RH7777 was purchased from the American Type Culture Collection (CRL-1601; ATCC, Manassas, VA) and maintained in Dulbecco's modified Eagle medium (DMEM; Mediatech, Herndon, VA) supplemented with 10% heat-inactivated fetal bovine serum (FBS; Sigma-Aldrich, St. Louis, MO) in a humidified atmosphere containing 5% CO_2 at 37°C. Cells were washed three times with phosphate-buffered saline (PBS) for a final concentration of 4×10^6 cells/20 μl before injection into rat liver. For virus infectivity assays, McA-RH7777 cells were seeded at 5×10^4 cells per well in a 24-well plate overnight. The next day, cells were infected in triplicate with VSV-hIFNβ, VSV-mIFNβ, or VSV-rIFNβ at the following multiplicities of infection (MOIs): 0, 0.0001, 0.001, 0.01, 0.1, 1, and 10 in Opti-MEM (Invitrogen, Carlsbad, CA). After 2 hr, inoculum was replaced with normal culture medium. At 48 hr, cell viability was determined by trypan blue exclusion assay.

Source of test article

The construction of VSV-mIFNβ and VSV-hIFNβ has been described previously (Obuchi *et al.*, 2003). A recombinant VSV expressing rat IFN-β was generated by polymerase chain reaction (PCR) cloning of rat IFN-β cDNA into the full-length infectious cDNA clone of VSV-hIFNβ, thus replacing the human IFN-β cDNA. VSV-hIFNβ and VSV-rIFNβ were provided by the Mayo Clinic Viral Vector Production Laboratory.

Viruses were frozen at −65°C or lower until use. Virus was diluted in sterile normal saline to the designated dose level and kept on ice until administration to animals. Virus dose was verified by 50% tissue culture infective dose ($TCID_{50}$) titration on Vero cells postadministration to animals.

In-life studies in rodents

All procedures involving animals were reviewed and approved by the Mayo Clinic Animal Use and Care Committee. Male and female Harlan Sprague Dawley (HSD) rats (Harlan Laboratories, Madison, WI) or Buffalo rats (Charles River, Wilmington, MA) were microchipped and ear-notched for identification. Rats were between 6 and 9 weeks of age on the day of article injection. On the day of surgery, rats were administered buprenorphine (0.1 mg/kg) in saline subcutaneously. Inhalant isoflurane was administered with an E-Z Anesthesia small animal system (Euthanex/E-Z Systems, Palmer, PA) to anesthetize the rats during surgery. Test or control article was injected into the left lateral lobe of rat liver on day 0. The surgical procedure is described as follows. A midline incision was made approximately 1 cm directly below the xiphoid process and approximately 2–3 cm in length. The left lateral lobe of the liver was exposed and slowly injected with 50–100 μl of VSV-hIFNβ or VSV-rIFNβ or 50–100 μl of saline, using a 28-gauge 0.5-inch needle. Direct pressure was applied to the injection site, using a sterile cotton-tipped applicator, immediately after withdrawal of the needle to prevent leakage and bleeding. The peritoneal and abdominal incisions were sutured with 6-0 or 4-0 coated Vicryl, and the skin was secured with 9-mm Clay auto-clips. The closed incision was coated with triple antibiotic ointment. Skin clips were removed 10–14 days postsurgery. Rats were monitored for abnormal clinical signs related to viral toxicity/neurotoxicity. Body weights were measured daily for the first week, and thereafter weekly out to preselected time points (day 44 or day 91), at which time scheduled euthanasia was performed.

To establish the orthotopic syngeneic rat HCC xenograft model, Buffalo rats (Charles River) were injected with McA-RH7777 cells intrahepatically 11 days (day –11) before the start of the study (Fig. 1). Rats were anesthetized and an incision was made as described previously. The left lateral lobe of the liver was exposed and slowly injected with 20 μl of McA-RH7777 cells, using a 28-gauge 0.5-inch needle. Cautery was applied, using an ACCU-TEMP high-temperature cautery (Medtronic Ophthalmics, Jacksonville, FL), to the injection site immediately after withdrawal of the needle to prevent cell leakage and bleeding. The incisions were sutured and closed as described previously. On study day 0, skin clips were removed and the surgical wound was

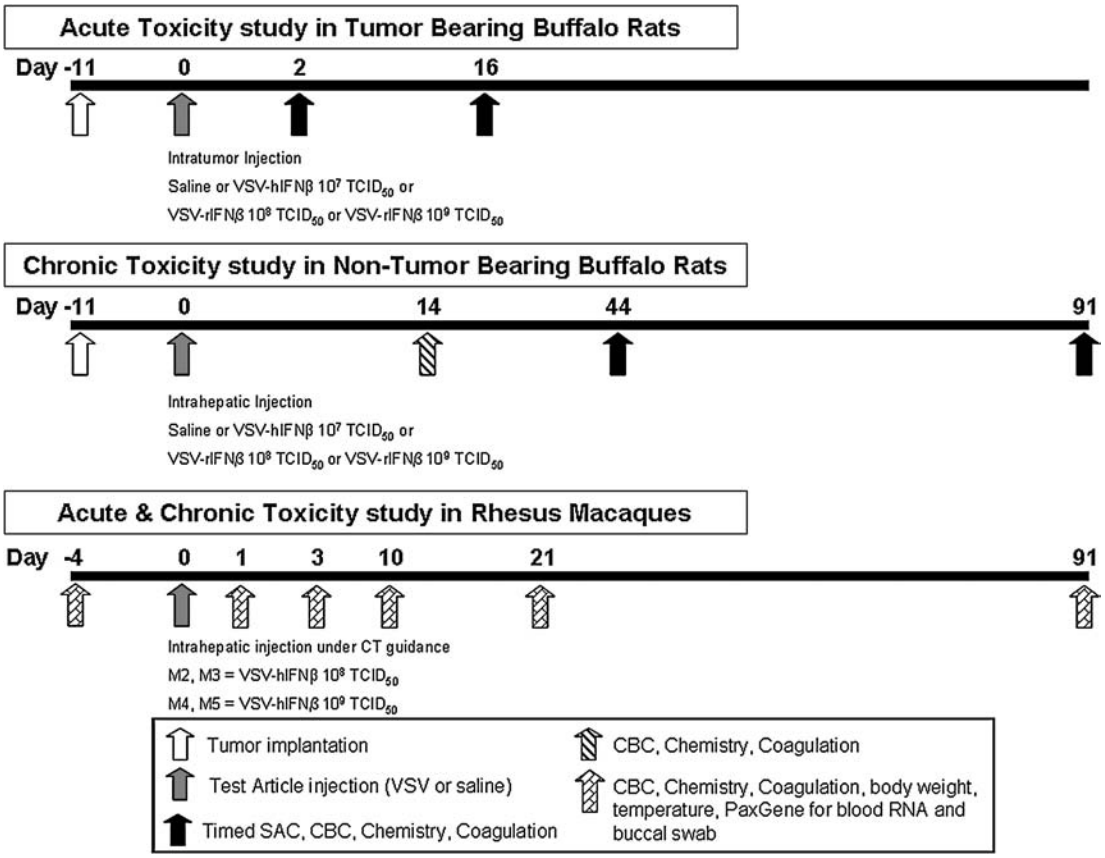

FIG. 1. Schema of toxicity studies in Buffalo rats and rhesus macaques. Buffalo rats were surgically implanted with an orthotopic syngeneic hepatocellular carcinoma (McA-RH7777) tumor 11 days before test article administration in the acute toxicity studies. CBC, complete blood count; SAC, sacrifice; $TCID_{50}$, 50% tissue culture infective dose; VSV-hIFNβ, vesicular stomatitis virus expressing human interferon-β; VSV-rIFNβ, vesicular stomatitis virus expressing rat interferon-β.

reopened to visualize the tumor and the tumor was injected with the test or control article (50–100 μl, depending on the study), using a 28-gauge 0.5-inch needle. In rats with disseminated tumors involving more than one tumor nodule, the predominant primary tumor in the left lateral lobe of the liver was injected.

In-life studies in nonhuman primates

All procedures involving animals were reviewed and approved by the Mayo Clinic Animal Use and Care Committee. Four adult rhesus macaques (*Macaca mulatta*) were obtained from Alpha Genesis (Yemassee, SC). Macaques were examined regularly by the attending veterinarians and were healthy and seronegative for herpesvirus B and VSV before the start of the study. Four days before the start of the study, macaques were bled (by femoral vein puncture) and their complete blood count (CBC), coagulation, and clinical chemistry parameters were measured. In addition, buccal swabs and blood were collected for quantitative real time PCR (qRT-PCR) for viral nucleocapsid (N) mRNA. Body temperatures and weights were also obtained at these time points.

CT-guided intrahepatic injection of VSV-hIFNβ

Before VSV injection, macaques were fasted for 12 hr and anesthetized with ketamine (8–24 mg/kg) and xylazine (0.5–2.0 mg/kg) given intramuscularly. Macaques were intubated and placed on 1.5% isoflurane with a 2.5-liter/min flow rate of O_2. Before injection, noncontrast localization CT images were obtained through the macaque liver. The images were reviewed by a board-certified interventional radiologist and no abnormalities were detected. A metallic marker was placed on the macaque's skin over the region of the left hepatic lobe, using CT image guidance. Under sterile conditions, a 25-gauge needle was then inserted 2 cm into the left hepatic lobe at the marked location. After needle placement, CT images were obtained to document correct needle position. One milliliter of test article VSV-hIFNβ was injected slowly through the needle over 10 sec. The needle was removed 10 sec after injection, the injection site was cleaned with sterile saline, and a bandage was applied. Postinjection CT images were obtained and showed no evidence of bleeding or other procedure-related complications.

Blood collection and analysis

Rats were bled 0.4 ml by the venous retro-orbital plexus of the eye (1 hr, day 1) or by nonterminal cardiac heart stick (remainder of the study) under general isoflurane anesthesia. Macaques were bled 3–5 ml by femoral vein puncture, after sedation with ketamine. For hematology studies, blood was collected into EDTA Vacutainer or Microtainer tubes (BD Diagnostic Systems, Sparks, MD). Blood samples were analyzed for CBC with a VetScan HM2 hematology system (Abaxis, Union City, CA) to provide data on hemoglobin, red blood cell count, hematocrit, mean corpuscular volume, mean corpuscular hemoglobin concentration, red cell distribution width, white blood cell count, lymphocytes, monocytes, granulocytes, platelet count, plateletcrit, mean platelet volume, and platelet distribution width. For coagulation assays, blood was collected into sodium citrate tubes (final concentration, 10% sodium citrate in sample). Forty microliters was analyzed on citrate PT (prothrombin) cartridges and 40 μl was analyzed on citrate APTT (activated partial thromboplastin time) cartridges with an SCA2000 veterinary coagulation analyzer (Synbiotics, Kansas City, MO). For clinical chemistry assays, lithium heparinized whole blood was analyzed on a VetScan chemistry analyzer with comprehensive diagnostic profile (Abaxis). Clinical chemistry data included albumin, alkaline phosphatase, alanine aminotransferase, amylase, total bilirubin, blood urea nitrogen, calcium, phosphorus, creatinine, glucose, sodium, potassium, total protein, and globulin. Means and standard deviations were calculated and plotted with GraphPad Prism version 4.00 (GraphPad Software, San Diego, CA). Creatinine readouts of <0.2 mg/dl (limit of detection) were calculated as 0.1 mg/dl for plotting and statistical analysis purposes.

Virus recovery from tissues

Samples were collected and frozen at -65°C or lower until use. Tissues were weighed and homogenized in 3 volumes (w/v) of Opti-MEM buffer. The supernatant was clarified by centrifugation and 10-fold serial dilutions of samples were prepared in Opti-MEM. Aliquots (50 μl) of each dilution were placed in 96-well plates containing Vero cells and $TCID_{50}$ titrations were performed as described previously (Hadac *et al.*, 2004).

RNA isolation from buccal swabs and from peripheral blood mononuclear cell samples

Approximately 2.5 ml of whole blood was collected into a PAXgene collection tube and processed according to the instructions of the manufacturer (Qiagen, Valencia, CA), using a PAXgene blood RNA kit (Qiagen) with the optional on-column DNase treatment. Buccal swabs were obtained by swabbing each macaque's buccal mucosa, using 10 firm back-and-forth motions, with a sterile Omni Swab (cat. no. WB100035; Whatman Biosciences/GE Healthcare Biosciences, Piscataway, NJ). The swabs were ejected into 400 μl of buffer RLT (plus 2-mercaptoethanol) and placed on ice for up to 90 min. Samples were processed as per the instructions of the manufacturer (Qiagen). RNA was quantitated by spectroscopy and frozen at -65°C or lower until further analysis by qRT-PCR.

qRT-PCR for VSV nucleocapsid mRNA

The final 50-μl reaction contained 300 n*M* forward primer (5′-TGATAGTACCGGAGGATTGACGAC-3′), 250 n*M* dual-labeled probe (5′-FAM-TCGACCACATCTCTGCCTT GTGGCGGTGCA-BHQ-3′), and 300 n*M* reverse primer (5′-CCTTGCAGTGACATGACTGCTCTT-3′); 2$\times$ one-step RT-PCR master mix and 40$\times$ MultiScribe/RNase inhibitor (kit 4309169; Applied Biosystems, Foster City, CA); nuclease-free water; and RNA template. One cycle of reverse transcription reaction (10 min at 48°C) was applied, followed by a denaturation step (10 min at 95°C) and 40 cycles of amplification (15 sec at 95 °C and 60 sec at 60°C). Fluorescence was measured at the annealing/extension step on an Mx4000 multiplex quantitative PCR system (Stratagene/Agilent Technologies, La Jolla, CA). Whenever possible, tissue RNA samples were diluted to 0.2 μg per reaction. Samples were quantitated by comparison with a standard curve generated by amplification

of 432-bp *in vitro*-transcribed RNA (MAXIscript SP6 kit; Ambion/Applied Biosystems, Austin, TX) encoding a 298-base portion of the VSV nucleocapsid gene (bases 972–1269) cloned in pCRII-TOPO (Invitrogen). All samples and standards were run in triplicate.

VSV plaque reduction neutralization assay

Macaque sera were diluted with phosphate-buffered saline (PBS) in a volume of 50 μl in serial 2-fold dilutions in triplicate in 96-well plates. A total of 50 μl of each virus (approximately 300 $TCID_{50}$) in Opti-MEM I reduced-serum medium was added to the diluted serum in each well. The 96-well plates containing serum and virus were incubated at 37°C for 1 hr. Approximately 4000 Vero cells in 50 μl of Opti-MEM were then added to each well. The plates were incubated at 37°C with 5% CO_2 for 2 hr. Fifty microliters of Dulbecco's modified Eagle's medium supplemented with 5% fetal bovine serum was added to each well. The plates were incubated at 37°C with 5% CO_2 for 2 to 3 days. Neutralizing titers are given as the highest dilutions that corresponded to complete inhibition of VSV cytopathic effect.

Rhesus plasma cytokine levels

Rhesus plasma interleukin (IL)-6 levels were assayed with a human IL-6 enzyme-linked immunoassay (ELISA) kit as per the instructions of the manufacturer (R&D Systems, Minneapolis, MN). Cross-reactivity of rhesus and human IL-6 is 98% (Villinger *et al.*, 1995). Rhesus plasma tumor necrosis factor (TNF)-α levels were assayed with a rhesus-specific TNF-α ELISA kit as per the instructions of the manufacturer (R&D Systems). The level of human IFN-β transgene expression was measured in plasma harvested on day –4 prestudy or at various time points after virus administration, using a human IFN-β ELISA kit as per the manufacturer's instructions.

Results

Intravenous, intrahepatic, and intracerebral administration of VSV-mIFNβ to BALB/c mice

In pilot studies using BALB/c mice, we found that intravenous administration of 10^{10} $TCID_{50}$ of VSV-mIFNβ resulted in neurotoxicity, occurring between days 2 and 7, manifested as seizures, whole body tremors, and weight loss of 10% on day 1. Infectious virus was recovered by overlay of brain homogenates on Vero cells. BALB/c mice ($n = 16$) given 10^8 or 10^9 $TCID_{50}$ of VSV-mIFNβ intravenously did not exhibit neurological symptoms, although animals appeared scruffy and lost 6–16% of initial body weight between days 1 and 7. Animals apparently recovered from the infection by day 9, with no clinical symptoms until the end of the study (2 months). Direct intrahepatic administration of VSV-mIFNβ at doses of 10^9 $TCID_{50}$ required euthanasia of 2 of 12 BALB/c mice because of neurotoxicity. One mouse was found dead 1 day after virus administration and the other mouse was lethargic with labored respiration on day 2. Hind limb paralysis set in by day 5 and this mouse was euthanized. Its serum ALT level was three times higher than normal at euthanasia and infectious virus was recovered from the brain by overlay of brain homogenate on Vero cells.

VSV-mIFNβ was also injected directly into the brains of BALB/c mice, using a Hamilton syringe fitted to a small animal stereotactic frame. As expected, direct intracerebral injection of VSV-mIFNβ (10^7 $TCID_{50}$) resulted in neurotoxicity in 100% of mice ($n = 8$). Clinical signs became obvious by day 2, which included weight loss, hunched posture, scruffy coat, lateral recumbency, and paraphimosis. Animals were euthanized by day 4. Mice given 10^4 $TCID_{50}$ of VSV-mIFNβ (5 of 6 mice) or 10^3 $TCID_{50}$ of VSV-mIFNβ (6 of 12 mice) also exhibited neurotoxic signs by days 3–4, including scruffy coat, hind limb paralysis, and paraphimosis. At 10^2 $TCID_{50}$, 2 of 11 mice were euthanized because of neurotoxicity. Thus, mice typically exhibited neurotoxic signs early on days 1–2 and were euthanized by days 4–6. The rest of the mice remained symptom-free until the end of the study (day 15 or 94).

Changes in hematology, clinical chemistry, and coagulation parameters after intrahepatic injection of test article VSV-hIFNβ into HSD rats

The test article or saline control was injected into the left lateral lobe of surgically exposed livers of HSD rats (six males and six females per treatment group). The rats received 100 μl of undiluted VSV-hIFNβ at the highest available dose (7.59×10^9 $TCID_{50}$/rat) at the time of study. The rats recovered well from the surgery. The HSD rats tolerated 7.59×10^9 $TCID_{50}$ of VSV-hIFNβ well and there were no clinical symptoms or adverse events observed from day 0 to the end of the study on day 28. Rats from each treatment group were divided into two cohorts (three females and three males per cohort) and each cohort was alternately bled via the retro-orbital plexus (at 1 hr and day 1 after virus administration) or via nonterminal cardiac puncture (days 2–28) to monitor acute or subacute changes in hematology, coagulation, and clinical chemistry parameters.

The total white blood cell count (WBC) was lower in rats receiving VSV-hIFNβ on day 1, with a concurrent decrease in lymphocyte percentage and an increase in the percentage of granulocytes (Fig. 2). This was resolved by day 2. Platelet count (Plt) and plateletcrit (Pct) decreased 2-fold by days 1–3, but returned to control levels by day 4 (Fig. 2). Other hematology parameters showed no difference between control and experimental rats (data not shown).

Analysis of plasma clinical chemistries indicated that there was a trend, although not statistically significant, for rats receiving VSV-hIFNβ to show higher levels of alanine aminotransferase (ALT) and alkaline phosphatase (ALP) on days 2 and 3 after test article administration (Fig. 2). Total bilirubin was stable (data not shown). Albumin levels decreased for both saline- and virus-treated groups, likely due to the surgical procedure, but recovered to pretreatment levels by day 7 (Fig. 2). There was no lengthening of prothrombin times, but activated partial thromboplastin (APTT) was transiently lengthened on day 1 (concurrent with platelet depression), with recovery by day 2 for rats receiving VSV-hIFNβ (Fig. 2).

Maximal tolerated dose of VSV-hIFNβ and VSV-rIFNβ in Buffalo rats without or with orthotopic HCC xenografts

Rat HCC McA-RH7777 cells were highly susceptible to VSV-hIFNβ and VSV-mIFNβ, with significant (>80%) cell

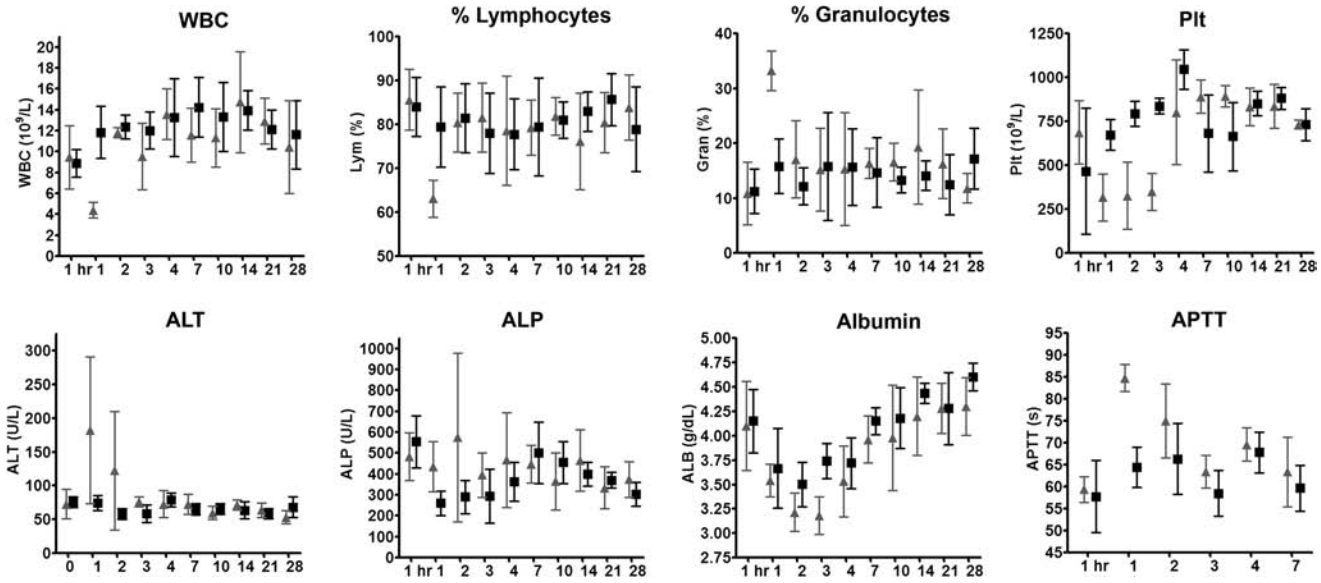

FIG. 2. Profiles of selected blood parameters over time after intrahepatic administration of saline (solid squares) or 7.59×10^9 $TCID_{50}$ of VSV-hIFNβ (shaded triangles) into Harlan Sprague Dawley rats. Each cohort of rats was alternately bled via the retro-orbital plexus (at 1 hr and day 1) or via nonterminal cardiac puncture (days 2–28) to monitor acute or subacute changes in hematology, coagulation, and clinical chemistry parameters. ALP, alkaline phosphatase; ALT, alanine aminotransferase; APTT, activated partial thromboplastin time; Plt, platelet count; WBC, white blood cell count.

death at 48 hr at low MOI (Fig. 3). These cells were also susceptible to infection and cell killing by VSV-rIFNβ, but cell killing required a higher MOI because the rat cells were protected by the antiviral effects of rIFN-β (Fig. 3).

Preliminary dose-finding studies were performed in tumor-free and tumor-bearing Buffalo rats. Increasing doses of VSV-hIFNβ or VSV-rIFNβ were injected into the left hepatic lobe or into orthotopic McA-RH7777 tumors. Higher doses of VSV-hIFNβ were associated with neurotoxicity, presented typically as hind limb or sometimes fore limb paralysis in rats; 5 of 6 tumor-free rats and 19 of 44 tumor-bearing rats that received 7.59×10^9 $TCID_{50}$ of VSV-hIFNβ (maximal feasible dose) were killed between days 2 and 9 after virus injection because of partial or complete paralysis of limbs. In contrast, 1 of 6 tumor-free rats (killed on day 8) and 1 of 11 tumor-bearing rats (killed on day 26) that received the lower dose of 7.59×10^7 $TCID_{50}$ of VSV-hIFNβ exhibited neurotoxicity (limb paralysis). In addition to paralysis of limbs, other typical clinical symptoms included weight loss and porphyrin staining, an indicator of stress, around the eyes and nares of affected animals. Head tilt, circling, and/or ataxia were seen in some rats. Brains and tumors harvested from animals that showed neurotoxic signs stained positive in immunohistochemistry for VSV antigen (Fig. 4). Virus was recovered by overlay of homogenates of tumors and brains, but not livers, of paralyzed rats on Vero cells (Fig. 4). ELISA analysis showed high levels of hIFN-β in the conditioned medium of infected Vero cells, confirming the integrity of the hIFN-β transgene in viruses recovered from the brain tissues (data not shown). Quantitative RT-PCR for VSV nucleocapsid (N) mRNA indicated abundant viral mRNA (1.3×10^9 copies of VSV-N mRNA per microgram of RNA; range, 1.2×10^4 to 8.0×10^9; $n=9$) in the brains of animals that were euthanized because of neurological symptoms (Fig. 4). In contrast, qRT-PCR for VSV-N mRNA in the liver detected only $1.5–2.5\times10^3$ copies of VSV-N mRNA per microgram of RNA (Fig. 4). Liver sections from rat 7 and rat 8 stained negative for VSV-N protein (Fig. 4).

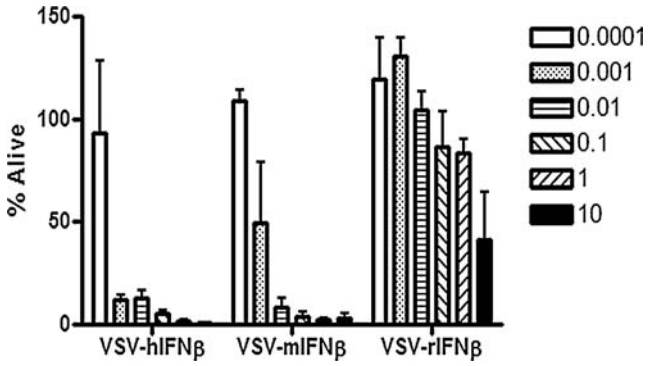

FIG. 3. Viability of Buffalo rat HCC cell line McA-RH7777 postinfection with VSV-hIFNβ, VSV-mIFNβ, or VSV-rIFNβ. Cells were infected with virus at various multiplicities of infection (MOIs) and cell viability was determined 48 hr later. Percent survival was determined by comparing the number of live cells in a mock-infected well with the number of live cells in the test well. Data shown represent the average of three replicates; error bars denote the SD.

The maximal tolerated dose (MTD) of VSV-rIFNβ was significantly higher than that of VSV-hIFNβ in these Buffalo rats. No adverse events were observed in virus-treated tumor-free or tumor-bearing rats even at the highest dose of VSV-rIFNβ virus tested (10^{10} $TCID_{50}$). All rats survived without clinical symptoms until the end of the study (day 90). From these studies, we conclude that the MTD was $<7.59\times10^7$ $TCID_{50}$ for VSV-hIFNβ and $>10^{10}$ $TCID_{50}$ for VSV-rIFNβ postinjection of the respective viruses into an orthotopic tumor nodule or into normal liver of Buffalo rats.

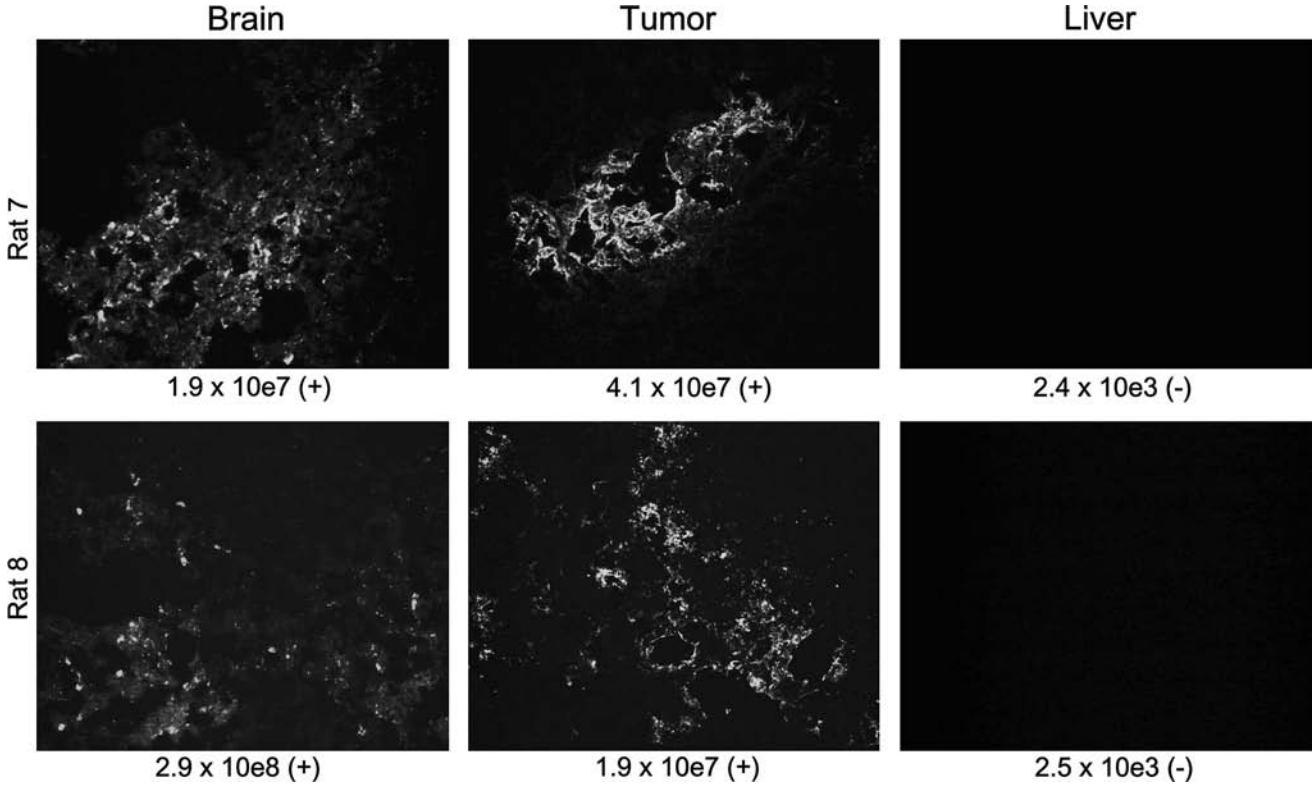

FIG. 4. Analyses of tissues harvested from rats that showed neurotoxic signs by immunohistochemistry for VSV nucleocapsid (N) protein. The corresponding amount of VSV-N mRNA in each organ was determined by quantitative RT-PCR for VSV-N mRNA and infectious virus was recovered by overlay of tissue homogenates on Vero cells. Copy number of N per microgram of RNA is indicated under each image and symbols in parentheses indicate the presence (+) or absence (–) of infectious virus recovered from the tissue homogenates.

From these preliminary studies, the estimated no observable adverse event levels (NOAELs) of VSV-hIFNβ and VSV-rIFNβ in Buffalo rats were 10^7 and 10^{10} $TCID_{50}$, respectively. As such, we chose to use 10^7 $TCID_{50}$ of VSV-hIFNβ and 10^8 and 10^9 $TCID_{50}$ of VSV-rIFNβ in our formal preclinical toxicology/pharmacology studies in support of the Investigational New Drug application to the FDA. McA-RH7777 is an aggressive orthotopic syngeneic HCC tumor xenograft model in Buffalo rats (Ebert *et al.*, 2003). Hence, only short-term toxicology/pharmacology studies (harvest, day 2 and days 14–16) can be performed in this model (Fig. 1). Saline, VSV-hIFNβ (10^7 $TCID_{50}$), or VSV-rIFNβ (two dose levels: 10^8 and 10^9 $TCID_{50}$) were injected into orthotopic tumors implanted 11 days previously in Buffalo rats (five female rats and five male rats per group per time point). Rats were euthanized on day 2 (acute toxicity study) and on days 14–16 (subacute toxicity study). A longer term toxicity study was also performed by injecting saline, VSV-hIFNβ, or VSV-rIFNβ into the left lateral lobe of normal livers of tumor-free Buffalo rats. These rats were harvested on day 44 (intermediate toxicity) and on day 91 (long-term toxicity).

A total of 40 Buffalo rats received VSV-hIFNβ (10^7 $TCID_{50}$ per rat) and 80 Buffalo rats received VSV-rIFNβ (2 dose levels, 10^8 or 10^9 $TCID_{50}$ per rat), and no adverse events were observed. In particular, no signs of neurotoxicity or weight loss of more than 10% were observed at any time point. Tissues (brain, tumor, liver, and spleen) harvested on day 2 from VSV-hIFNβ- and VSV-rIFNβ-treated animals were homogenized and virus yield was determined by $TCID_{50}$ titrations on Vero cells. Virus was recovered from tumors but not from liver, spleen, or brain on day 2 after virus injection (Fig. 5A). Virus recovered from tumors ranged from 2.53×10^3 to 8.01×10^6 $TCID_{50}$/g tumor (Fig. 5A). All tumors harvested on day 16 were negative for virus recovery. Quantitative RT-PCR analysis of VSV-N mRNA was performed on RNA extracted from blood (Fig. 5B) and tissues (Fig. 5C) harvested on day 2 postinjection of VSV-hIFNβ or VSV-rIFNβ. Viral RNA copy number was highly variable in tumors, ranging from 3.41×10^3 to 2.16×10^7 copies/μg RNA (Fig. 5C). Although VSV-N mRNA was detected in the spleen and liver parenchyma adjacent to the tumor nodule (Fig. 5C), no detectable infectious virus was recovered from spleen or liver.

RNA was isolated from the whole blood of treated rats and qRT-PCR was performed. Viremia was detected in rats injected with VSV-hIFNβ and VSV-rIFNβ on day 2, suggesting that the viruses could have infected lymphocytes and disseminated to distant sites via the bloodstream (Fig. 5B). Tumor, spleen, liver, and ovaries, but not testes, tested positive for VSV-N mRNA in tumor-bearing rats treated with VSV-hIFNβ (Fig. 5C). Other organs such as kidney, mesenteric lymph node, pancreas, eye, spinal cord, optic nerves, prostate, seminal vesicle, bone marrow, quadriceps, sciatic nerve, large intestine, stomach, bladder, lungs, heart, and thymus were negative for VSV-N mRNA in these tumor-bearing rats. The brains from all rats treated with VSV-hIFNβ

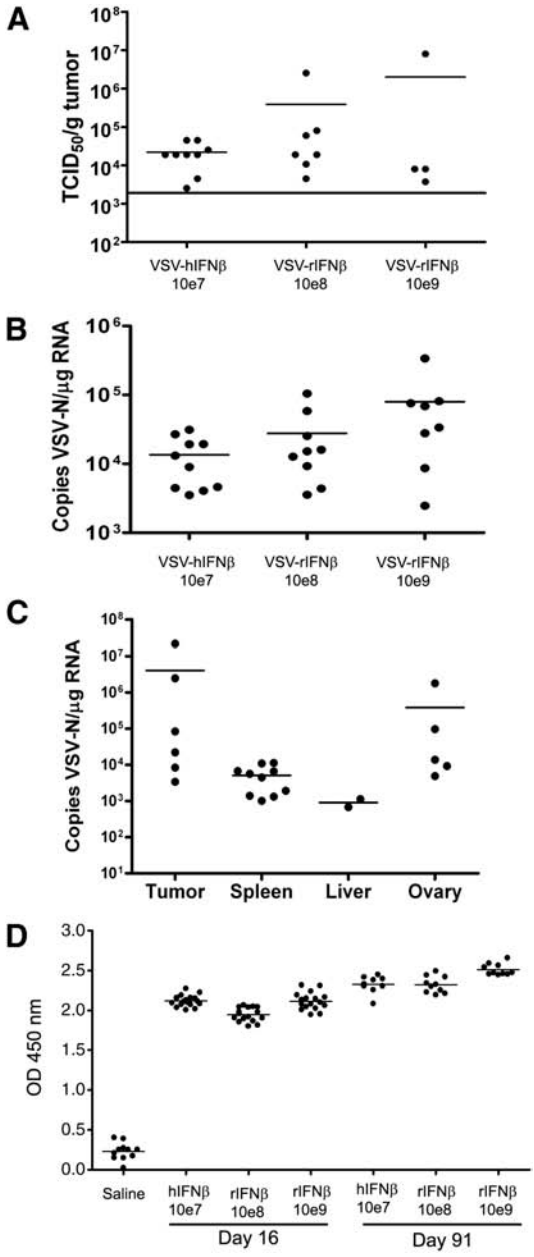

FIG. 5. Analyses of blood and tissues harvested from tumor-bearing or tumor-free Buffalo rats given VSV-hIFNβ (10^7 $TCID_{50}$) or VSV-rIFNβ (10^8 or 10^9 $TCID_{50}$). (**A**) Recovery of VSV from tumors harvested from rats on day 2 after intratumoral injection of respective viruses. Tumors were homogenized in Opti-MEM and $TCID_{50}$ titrations were performed on Vero cells. Any titer $<2\times10^3$ $TCID_{50}$/g tumor was below the limits of detection for this assay. (**B**) Quantitative RT-PCR results indicate the presence of viremia in the blood of rats on day 2 after intratumoral injection of the respective viruses. Data were calculated for copy number of VSV-nucleocapsid (N) RNA per microgram of total RNA isolated from whole blood. The limit of detection was 100 copies of VSV-N mRNA per 0.2 μg of RNA. (**C**) Quantitative RT-PCR results showing the presence of VSV-N RNA in tumor, spleen, liver, and ovary harvested on day 2 from rats that received an intratumoral injection of 10^7 $TCID_{50}$ of VSV-hIFNβ. (**D**) ELISA assay for anti-VSV antibodies in the sera of tumor-free rats on day 16 or 91 after intrahepatic administration of respective viruses.

(10^7 $TCID_{50}$) or VSV-rIFNβ (10^8 or 10^9 $TCID_{50}$) tested negative for VSV-N mRNA at all time points. There was a corresponding increase in anti-VSV neutralizing antibodies in the sera of rats that received VSV from day 16, day 44 (data not shown), and day 91 but not in saline-treated animals (Fig. 5D).

Intrahepatic injection of VSV-hIFNβ into rhesus macaques

Four adult male rhesus macaques were injected with 1 ml of VSV-hIFNβ via the left hepatic lobe under CT guidance by a board-certified interventional radiologist to ensure correct placement of the test article (Fig. 6). Macaques 5M02 and 5M03 received 10^9 $TCID_{50}$ of VSV-hIFNβ whereas macaques 5M04 and 5M05 received 10^{10} $TCID_{50}$ of VSV-hIFNβ on study day 0. The time between anesthesia and end of injection was 60 min. No bleeding was observed. After completion of the procedure, macaques were placed back in their home cage and observed periodically until they had recovered from anesthesia. All animals recovered well from the procedure. After treatment the macaques were observed a minimum of twice daily for 7 days, after which observations were performed once daily. No signs of neurotoxicity were observed. There were no abnormal changes in activity level, posture, facial symmetry, gait, behavior, motor function, or level of consciousness to date (1 year after virus administration).

At preselected time points of 1, 3, 10, 21, and 90 days after VSV injection (Fig. 1), animals were weighed and blood and buccal swabs were collected as scheduled (Fig. 1). No weight loss was seen throughout the study (Fig. 6). There were no significant changes in hematology parameters and clinical chemistries were within 1 standard deviation of the normal reference range for rhesus macaques (Fig. 6). The one exception was 5M05, which had higher levels of ALT before the start of the study, but the ALT levels had returned to within the standard range by day 20 and remained within the normal reference range until the end of the study.

qRT-PCR for VSV-N mRNA in blood and buccal swabs of macaques

RNA was isolated from whole blood and buccal swabs were collected prestudy (day –4) and poststudy (days 1, 3, 10, 21, and 91) from the macaques. No detectable levels of VSV-N mRNA were found in any of the blood and buccal swab samples prestudy. All buccal swab samples were negative for VSV-N mRNA after virus administration. The limit of detection was 100 copies of VSV-N mRNA per 0.2 μg of RNA. Most blood samples were also negative for viral genomes except for 5M03 and 5M05 on day 1 after virus delivery. Positive levels of viral RNA (3×10^3 copies of VSV-N per microgram of RNA) were detected on day 1 in the blood of one of the low-dose macaques (5M03) and on day 1 in the blood of one of the high-dose macaques (5M05; 1.9×10^5 copies of VSV-N per microgram of RNA). No viral genomes were detected on day 3 or any of the later time points.

Cytokine levels in macaque sera

To determine whether there could be an induction of proinflammatory cytokines after virus administration, levels of IL-6 and TNF-α in sera were tested by ELISA. Rhesus plasma

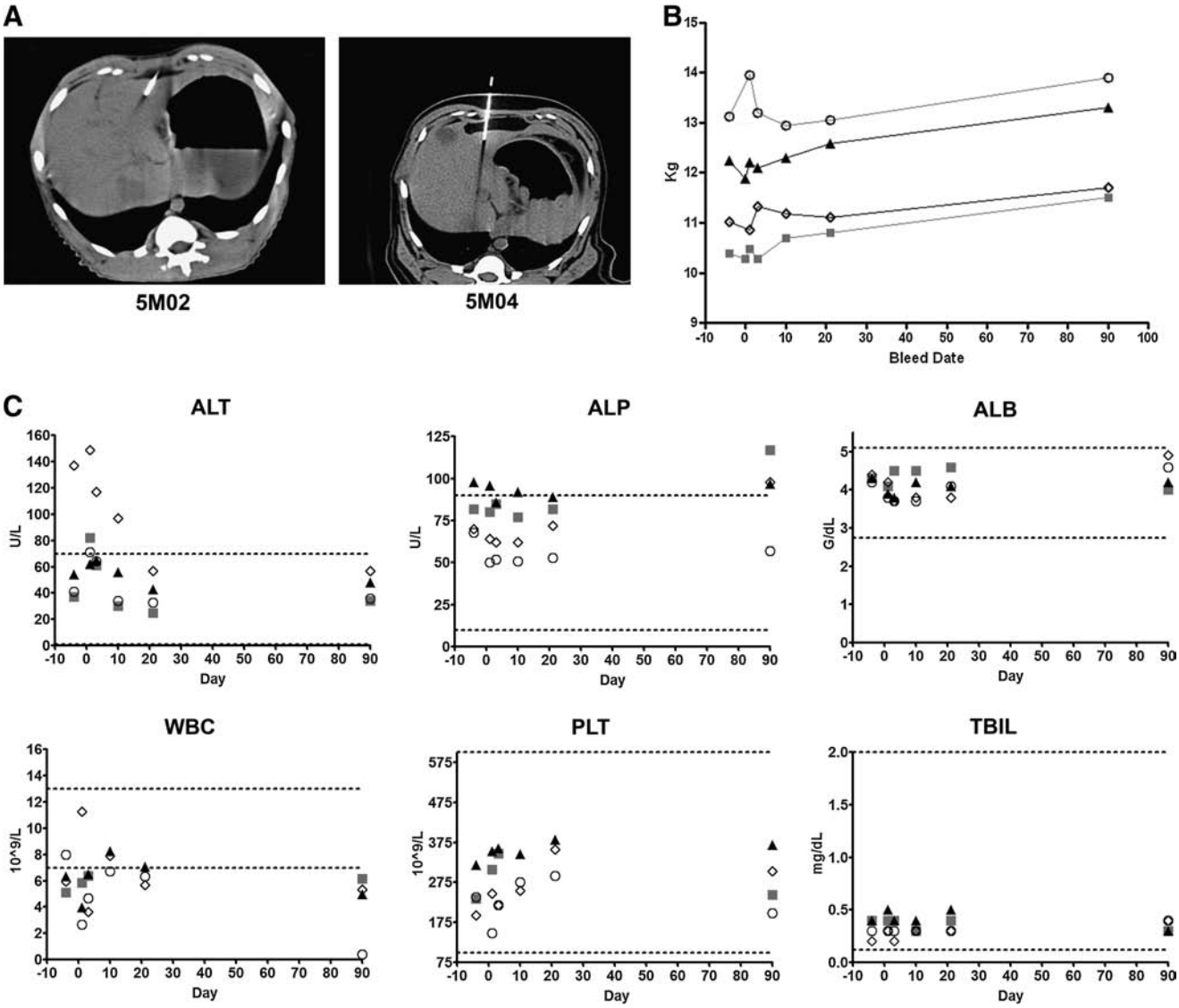

FIG. 6. Profiles of body weight and selected blood parameters of rhesus macaques injected intrahepatically with 10^9 $TCID_{50}$ (animals 5M02 and 5M03) or 10^{10} $TCID_{50}$ (animals 5M04 and 5M05) of VSV-hIFNβ. (**A**) Representative CT images showing virus administration into the hepatic lobes of 5M02 and 5M04. (**B**) Measurements of body weight over time, taken on day 4 prestudy or after viral administration. (**C**) A selection of measured blood analytes is shown. ALT, alanine aminotransferase; ALP, alkaline phosphatase; ALB, albumin; WBC, white blood cells; PLT, platelets; TBIL, total bilirubin. Dotted lines represent normal reference ranges of rhesus macaques. Shaded squares, 5M02; solid triangles, 5M03; open circles, 5M04; open diamonds, 5M05.

IL-6 levels were assayed with a human IL-6 immunoassay ELISA kit. Cross-reactivity of rhesus and human IL-6 is 98% (Villinger *et al.*, 1995). Rhesus plasma TNF-α levels were assayed with a rhesus-specific TNF-α ELISA. There were no detectable levels of TNF-α (<15.6 pg/ml) or IL-6 (<3.12 pg/ml) in the sera of macaques at any time point. The level of human IFN-β transgene expression was measured with a human IFN-β ELISA kit. No detectable levels of hIFN-β (<50 pg/ml) were found in the sera at any time point.

VSV plaque reduction neutralization assay

The amount of macaque plasma required to completely neutralize the cytopathic activity of 300 $TCID_{50}$ of VSV-hIFNβ virus was determined on Vero cells. Complement activity in all serum samples was heat-inactivated by incubation of samples at 55°C for 30 min before use in the plaque reduction neutralization (PRN) assay. As shown in Table 1, sera harvested prestudy and on days 1 and 3 after virus administration were negative for anti-VSV antibodies (<1:50 dilution). However, there was an increase in anti-VSV antibodies with time, increasing to 1:6400 serum dilution (highest dilution tested). Macaques treated with the higher dose virus had higher levels of anti-VSV antibodies that remained high at the end of the study on day 91.

Discussion

Oncolytic VSVs derived from the Indiana strain have shown promising antitumor activities against a variety of

Table 1. Titers of Anti-Vesicular Stomatitis Virus Antibodies in Macaque Plasma as Determined by Plaque Reduction Neutralization Assay

	Rhesus macaque ID			
Study day	*5M02*	*5M03*	*5M04*	*5M05*
−4	<50	<50	<50	<50
1	<50	<50	<50	<50
3	<50	<50	<50	<50
10	800	400	1600	3200
21	1600	1600	3200	6400
90	200	800	3200	6400

murine and human tumor xenografts (Barber, 2004; Lun *et al.*, 2006; Altomonte *et al.*, 2008; Nguyen *et al.*, 2008; Qiao *et al.*, 2008). To enhance the oncolytic potency of VSV, investigators have genetically modified the virus to express a variety of transgenes such as chemokine-binding protein, IL-12, and fusogenic glycoproteins (Ebert *et al.*, 2004; Shin *et al.*, 2007; Wu *et al.*, 2008). In addition, Goel and colleagues have demonstrated that addition of the human thyroidal sodium iodide symporter gene to the VSV genome permits radioiodine imaging of the sites of viral infection as well as enhancement of the antitumor activity of VSV by using ^{131}I, a β particle-emitting radionuclide (Goel *et al.*, 2007). Although there has been intensive preclinical work developing VSV for cancer therapy, clinical translation of VSV has lagged behind, mainly because of concerns about the neurovirulence of VSV when administered to animals (Clarke *et al.*, 2006). Documented cases of VSV infection of humans are rare and are not associated with encephalitis (Clarke *et al.*, 2006). Infection is typically subclinical or manifests as a mild flulike disease that is self-limiting (Clarke *et al.*, 2006). However, VSV causes fatal neurotoxicity when administered intracerebrally to rodents, cattle, goats, and nonhuman primates (Clarke *et al.*, 2006; Johnson *et al.*, 2007). Because VSV is exquisitely sensitive to the antiviral effects of type I interferon, development of interferon-inducing or interferon-expressing VSV has been the primary engineering strategy to attenuate neurovirulence of oncolytic VSV (Russell and Peng, 2007). Investigators generated recombinant VSV that expresses the IFN-β gene (Obuchi *et al.*, 2003) or matrix (M) protein mutants of VSV that are unable to suppress cellular innate immunity (Stojdl *et al.*, 2003; Ahmed *et al.*, 2008). Production and release of interferon-β from the virally infected cell generates an "interferon cloud" that alerts surrounding cells by activating the type I interferon-α/β receptor on the cells, and activating the Jak/Stat pathways to induce interferon and interferon-responsive genes (Garcia-Sastre and Biron, 2006). The end result of the type I interferon-initiated response is a decline in protein synthesis and the cell becoming an unfavorable host that limits viral replication and spread (Russell and Peng, 2007). This innate interferon response, although fully operational in primary cells, is often not functional in transformed tumor cells. Hence, VSV selectively replicates in many transformed cells (Barber, 2005).

Rodents and nonhuman primates have been used experimentally to study neurovirulence of VSV and its recombinants. Intranasal instillation of VSV into mice leads to initial infection of olfactory receptor neurons and then the olfactory bulb, and this is followed by acute infection of the CNS, breakdown of the blood–brain barrier, and the death of mice (Forger *et al.*, 1991; Bi *et al.*, 1995). Data indicate that attenuation of VSV can occur through genetic modifications of the viral genome (Cooper *et al.*, 2008). Thus, although all four cynomolgus macaques inoculated intrathalamically with 10^7 PFU of wild-type VSV developed signs of neurological disease by days 6–7 after virus inoculation (head tilt, irregular gait, tremors, and ataxia), only one of four macaques receiving recombinant VSV developed clinical and histological signs similar to the wild-type VSV group (Johnson *et al.*, 2007). The incidence of neurovirulence depends on the route of virus administration. No adverse clinical signs were observed where high doses of VSV were given intranasally or intramuscularly to more than 150 rhesus macaques (Johnson *et al.*, 2007).

Because the proposed route of VSV administration for the clinical trial is ultrasound-guided injection of VSV into an HCC nodule in the liver, we performed preclinical toxicology and pharmacology studies using intrahepatic or intratumoral injection of the vehicle control and test article in BALB/c mice and two rat strains: Harlan Sprague Dawley and Buffalo rats. Because human IFN-β is not biologically active in rodents, recombinant VSVs expressing murine IFN-β or rat IFN-β were generated and used in these studies. An important note from these studies is that insertion of the IFN-β gene did not totally abrogate neurovirulence of the recombinant VSV. For example, 2 of 12 BALB/c mice injected intrahepatically with 2.95×10^9 $TCID_{50}$ of VSV-mIFNβ exhibited neurotoxic signs. Brain, but not liver, tissue harvested from one of mice was positive for infectious virus in overlay cultures. It appears that although VSV-mIFNβ spread in the liver might be restricted by expression of the IFN-β gene, the brain is especially susceptible and highly permissive to VSV replication, despite the presence of IFN-β in the viral genome.

However, studies in HSD and Buffalo rats comparing intrahepatic injection of VSV-hIFNβ and VSV-rIFNβ indicated that expression of species-specific (rat) IFN-β can protect the host animal to a significant degree. The NOAEL of VSV in Buffalo rats was 10^7 $TCID_{50}$ for VSV-hIFNβ and 10^{10} $TCID_{50}$ for VSV-rIFNβ (highest dose tested). The dose of 10^{10} $TCID_{50}$/300-g rat translates to a human equivalent dose (HED) of 2.3×10^{12} $TCID_{50}$ of VSV-expressing species-specific IFN-β in a 70-kg human. This is significantly higher than the NOAEL of 10^7 $TCID_{50}$ of VSV-hIFNβ in a 300-g rat, which translates to an HED of 2.3×10^{10} $TCID_{50}$ of VSV expressing human IFN-β. We also noted a strain difference in the susceptibility of HSD rats versus Buffalo rats to VSV. No adverse clinical symptoms were observed in Harlan Sprague Dawley rats given an intrahepatic dose of 7.59×10^9 $TCID_{50}$ of VSV-hIFNβ (highest dose tested) whereas the NOAEL of VSV-hIFNβ in Buffalo rats was 10^7 $TCID_{50}$.

Toxicology and pharmacology studies were performed in Buffalo rats after injection of the test article VSV-hIFNβ (10^7 $TCID_{50}$) and a VSV expressing species-specific rIFN-β (two dose levels: high dose, 10^9 $TCID_{50}$; low dose, 10^8 $TCID_{50}$) into normal liver and into an orthotopic HCC (McA-RH7777) tumor nodule to mimic the clinical scenario, in which the test article would be injected into a discrete HCC nodule under image guidance. No adverse clinical symptoms were observed in tumor-free or tumor-bearing rats given VSV-hIFNβ or VSV-rIFNβ at any time point, from a few

hours postinjection out to day 91. Infectious virus was recovered from tumor homogenates harvested on day 2 but not day 16 after virus inoculation. No infectious virus was recovered from the liver, brain, or spleen of animals on days 2 or 16. Anti-VSV antibodies in rat sera were undetectable in animals on day 2 but increased by day 16 and remained high in animals harvested on day 91. *In vitro* infection studies using VSV-hIFNβ, VSV-mIFNβ, and VSV-rIFNβ indicated that rat HCC McA-RH7777 cells were highly susceptible to killing by VSV-hIFNβ (10% alive at an MOI of 0.001) and VSV-mIFNβ (50% alive at an MOI of 0.001) but were only partially susceptible to the oncolytic activity of VSV-rIFNβ (50% alive at an MOI of 10). Indeed, these HCC tumor cells are not totally defective in their IFN signaling pathway (IFN sensitive) and can respond to rIFN-β. Hence, McA-RH7777 cells are only semipermissive to VSV-rIFNβ, thus requiring a significantly higher amount of virus to achieve a comparable level of cell killing. These HCC tumor cells reflect a likely scenario in the clinical setting, where it is expected that a percentage of human HCC would be able to respond to IFN-β (Murata *et al.*, 2006). Indeed, combination chemotherapy of HCC with IFN-α results in enhanced survival of patients with HCC (Damdinsuren *et al.*, 2007; Ueshima *et al.*, 2008).

Recombinant VSV is clearly a promising virus with potent antitumor activity and should be evaluated clinically. The NOAEL doses of VSV-hIFNβ were established in Buffalo rats (10^7 $TCID_{50}$/300-g rat) and HSD rats (at least 7.59×10^9 $TCID_{50}$/300-g rat). Rhesus macaques that received 10^9 or 10^{10} $TCID_{50}$ of VSV-hIFNβ injected under CT guidance showed no adverse effects at the end of the study, 12 months after virus administration. These preclinical toxicology and pharmacology studies support a cautious dose escalation study to determine the safety of VSV-hIFNβ in patients with HCC.

Acknowledgments

The authors are grateful to the pharmacology/toxicology personnel of the Office of Cellular, Tissue, and Gene Therapies (OCTGT) in the Center for Biologics Evaluation and Research (CBER) of the U.S. Food and Drug Administration (FDA) for their input on the design of the toxicology/pharmacology studies, the Mayo Clinic Viral Vector Production Laboratory for providing purified VSV (Kristen Langfield, Henry Walker, and Sharon Stephan), the quality assurance team for auditing the toxicology/pharmacology studies (Dr. Linda Gregory, Cindy Whitcomb, and Julie Sauer), Emily McLean for immunohistochemical staining, and Drs. Jennifer Altomonte and Oliver Ebert (Technical University of Munich) for expert advice on the Buffalo rat HCC xenograft model. This work was supported by funds from the Mayo Foundation and Mayo Clinic Comprehensive Cancer Center (CA15083-34C12).

Author Disclosure Statement

No competing financial interests exist.

References

Ahmed, M., Marino, T.R., Puckett, S., Kock, N.D., and Lyles, D.S. (2008). Immune response in the absence of neurovirulence in mice infected with M protein mutant vesicular stomatitis virus. J. Virol. 82, 9273–9277.

Altomonte, J., Braren, R., Schulz, S., Marozin, S., Rummeny, E.J., Schmid, R.M., and Ebert, O. (2008). Synergistic antitumor effects of transarterial viroembolization for multifocal hepatocellular carcinoma in rats. Hepatology 48, 1864–1873.

Barber, G.N. (2004). Vesicular stomatitis virus as an oncolytic vector. Viral Immunol. 17, 516–527.

Barber, G.N. (2005). VSV-tumor selective replication and protein translation. Oncogene 24, 7710–7719.

Bi, Z., Barna, M., Komatsu, T., and Reiss, C.S. (1995). Vesicular stomatitis virus infection of the central nervous system activates both innate and acquired immunity. J. Virol. 69, 6466–6472.

Blum, H.E. (2005). Hepatocellular carcinoma: Therapy and prevention. World J. Gastroenterol. 11, 7391–7400.

Clarke, D.K., Cooper, D., Egan, M.A., Hendry, R.M., Parks, C.L., and Udem, S.A. (2006). Recombinant vesicular stomatitis virus as an HIV-1 vaccine vector. Springer Semin. Immunopathol. 28, 239–253.

Cooper, D., Wright, K.J., Calderon, P.C., Guo, M., Nasar, F., Johnson, J.E., Coleman, J.W., Lee, M., Kotash, C., Yurgelonis, I., Natuk, R.J., Hendry, R.M., Udem, S.A., and Clarke, D.K. (2008). Attenuation of recombinant vesicular stomatitis virus-human immunodeficiency virus type 1 vaccine vectors by gene translocations and G gene truncation reduces neurovirulence and enhances immunogenicity in mice. J. Virol. 82, 207–219.

Damdinsuren, B., Nagano, H., Wada, H., Kondo, M., Ota, H., Nakamura, M., Noda, T., Natsag, J., Yamamoto, H., Doki, Y., Umeshita, K., Dono, K., Nakamori, S., Sakon, M., and Monden, M. (2007). Stronger growth-inhibitory effect of interferon (IFN)-β compared with IFN-α is mediated by IFN signaling pathway in hepatocellular carcinoma cells. Int. J. Oncol. 30, 201–208.

Ebert, O., Shinozaki, K., Huang, T.G., Savontaus, M.J., Garcia-Sastre, A., and Woo, S.L. (2003). Oncolytic vesicular stomatitis virus for treatment of orthotopic hepatocellular carcinoma in immune-competent rats. Cancer Res. 63, 3605–3611.

Ebert, O., Shinozaki, K., Kournioti, C., Park, M.S., Garcia-Sastre, A., and Woo, S.L. (2004). Syncytia induction enhances the oncolytic potential of vesicular stomatitis virus in virotherapy for cancer. Cancer Res. 64, 3265–3270.

Forger, J.M., III, Bronson, R.T., Huang, A.S., and Reiss, C.S. (1991). Murine infection by vesicular stomatitis virus: Initial characterization of the H-2^d system. J. Virol. 65, 4950–4958.

Garcia-Sastre, A., and Biron, C.A. (2006). Type 1 interferons and the virus–host relationship: A lesson in detente. Science 312, 879–882.

Goel, A., Carlson, S.K., Classic, K.L., Greiner, S., Naik, S., Power, A.T., Bell, J.C., and Russell, S.J. (2007). Radioiodide imaging and radiovirotherapy of multiple myeloma using VSV(Δ51)-NIS, an attenuated vesicular stomatitis virus encoding the sodium iodide symporter gene. Blood 110, 2342–2350.

Hadac, E.M., Peng, K.W., Nakamura, T., and Russell, S.J. (2004). Reengineering paramyxovirus tropism. Virology 329, 217–225.

Johnson, J.E., Nasar, F., Coleman, J.W., Price, R.E., Javadian, A., Draper, K., Lee, M., Reilly, P.A., Clarke, D.K., Hendry, R.M., and Udem, S.A. (2007). Neurovirulence properties of recombinant vesicular stomatitis virus vectors in non-human primates. Virology 360, 36–49.

Kamiyama, T., Nakanishi, K., Yokoo, H., Kamachi, H., Tahara, M., Suzuki, T., Shimamura, T., Furukawa, H., Matsushita, M., and Todo, S. (2009). Recurrence patterns after hepatectomy of

hepatocellular carcinoma: Implication of Milan criteria utilization. Ann. Surg. Oncol. 16, 1560–1571.

Kopecky, S.A., Willingham, M.C., and Lyles, D.S. (2001). Matrix protein and another viral component contribute to induction of apoptosis in cells infected with vesicular stomatitis virus. J. Virol. 75, 12169–12181.

Kottke, T., Diaz, R.M., Kaluza, K., Pulido, J., Galivo, F., Wongthida, P., Thompson, J., Willmon, C., Barber, G.N., Chester, J., Selby, P., Strome, S., Harrington, K., Melcher, A., and Vile, R.G. (2008). Use of biological therapy to enhance both virotherapy and adoptive T-cell therapy for cancer. Mol. Ther. 16, 1910–1918.

Lichty, B.D., Power, A.T., Stojdl, D.F., and Bell, J.C. (2004). Vesicular stomatitis virus: Re-inventing the bullet. Trends Mol. Med. 10, 210–216.

Llovet, J.M., Ricci, S., Mazzaferro, V., Hilgard, P., Gane, E., Blanc, J.F., De Oliveira, A.C., Santoro, A., Raoul, J.L., Forner, A., Schwartz, M., Porta, C., Zeuzem, S., Bolondi, L., Greten, T.F., Galle, P.R., Seitz, J.F., Borbath, I., Haussinger, D., Giannaris, T., Shan, M., Moscovici, M., Voliotis, D., and Bruix, J. (2008). Sorafenib in advanced hepatocellular carcinoma. N. Engl. J. Med. 359, 378–390.

Lun, X., Senger, D.L., Alain, T., Oprea, A., Parato, K., Stojdl, D., Lichty, B., Power, A., Johnston, R.N., Hamilton, M., Parney, I., Bell, J.C., and Forsyth, P.A. (2006). Effects of intravenously administered recombinant vesicular stomatitis virus ($VSV^{\Delta M51}$) on multifocal and invasive gliomas. J. Natl. Cancer Inst. 98, 1546–1557.

Murata, M., Nabeshima, S., Kikuchi, K., Yamaji, K., Furusyo, N., and Hayashi, J. (2006). A comparison of the antitumor effects of interferon-α and β on human hepatocellular carcinoma cell lines. Cytokine 33, 121–128.

Nguyen, T.L., Abdelbary, H., Arguello, M., Breitbach, C., Leveille, S., Diallo, J.S., Yasmeen, A., Bismar, T.A., Kirn, D., Falls, T., Snoulten, V.E., Vanderhyden, B.C., Werier, J., Atkins, H., Vaha-Koskela, M.J., Stojdl, D.F., Bell, J.C., and Hiscott, J. (2008). Chemical targeting of the innate antiviral response by histone deacetylase inhibitors renders refractory cancers sensitive to viral oncolysis. Proc. Natl. Acad. Sci. U.S.A. 105, 14981–14986.

Novella, I.S., Ball, L.A., and Wertz, G.W. (2004). Fitness analyses of vesicular stomatitis strains with rearranged genomes reveal replicative disadvantages. J. Virol. 78, 9837–9841.

Obuchi, M., Fernandez, M., and Barber, G.N. (2003). Development of recombinant vesicular stomatitis viruses that exploit defects in host defense to augment specific oncolytic activity. J. Virol. 77, 8843–8856.

Parkin, D.M., Bray, F., Ferlay, J., and Pisani, P. (2005). Global cancer statistics, 2002. CA Cancer J. Clin. 55, 74–108.

Qiao, J., Wang, H., Kottke, T., Diaz, R.M., Willmon, C., Hudacek, A., Thompson, J., Parato, K., Bell, J., Naik, J., Chester, J., Selby, P., Harrington, K., Melcher, A., and Vile, R.G. (2008). Loading of oncolytic vesicular stomatitis virus onto antigen-specific T cells enhances the efficacy of adoptive T-cell therapy of tumors. Gene Ther. 15, 604–616.

Russell, S.J., and Peng, K.W. (2007). Viruses as anticancer drugs. Trends Pharmacol. Sci. 28, 326–333.

Shin, E.J., Wanna, G.B., Choi, B., Aguila, D., III, Ebert, O., Genden, E.M., and Woo, S.L. (2007). Interleukin-12 expression enhances vesicular stomatitis virus oncolytic therapy in murine squamous cell carcinoma. Laryngoscope 117, 210–214.

Stojdl, D.F., Lichty, B.D., Tenoever, B.R., Paterson, J.M., Power, A.T., Knowles, S., Marius, R., Reynard, J., Poliquin, L., Atkins, H., Brown, E.G., Durbin, R.K., Durbin, J.E., Hiscott, J., and Bell, J.C. (2003). VSV strains with defects in their ability to shutdown innate immunity are potent systemic anti-cancer agents. Cancer Cell 4, 263–275.

Ueshima, K., Kudo, M., Nagai, T., Tatsumi, C., Ueda, T., Takahashi, S., Hatanaka, K., Kitai, S., Ishikawa, E., Inoue, T., Hagiwara, S., Minami, Y., and Chung, H. (2008). Combination therapy with S-1 and pegylated interferon α for advanced hepatocellular carcinoma. Oncology 75(Suppl. 1), 106–113.

Verslype, C., Van Cutsem, E., Dicato, M., Arber, N., Berlin, J.D., Cunningham, D., De Gramont, A., Diaz-Rubio, E., Ducreux, M., Gruenberger, T., Haller, D., Haustermans, K., Hoff, P., Kerr, D., Labianca, R., Moore, M., Nordlinger, B., Ohtsu, A., Rougier, P., Scheithauer, W., Schmoll, H.J., Sobrero, A., Tabernero, J., and van de Velde, C. (2009). The management of hepatocellular carcinoma: Current expert opinion and recommendations derived from the 10th World Congress on Gastrointestinal Cancer, Barcelona, 2008. Ann. Oncol. 20(Suppl. 7), vii1–vii6.

Villinger, F., Brar, S.S., Mayne, A., Chikkala, N., and Ansari, A.A. (1995). Comparative sequence analysis of cytokine genes from human and nonhuman primates. J. Immunol. 155, 3946–3954.

Wu, L., Huang, T.G., Meseck, M., Altomonte, J., Ebert, O., Shinozaki, K., Garcia-Sastre, A., Fallon, J., Mandeli, J., and Woo, S.L. (2008). rVSV(MΔ51)-M3 is an effective and safe oncolytic virus for cancer therapy. Hum. Gene Ther. 19, 635–647.

Address correspondence to:
Dr. Kah-Whye Peng
Department of Molecular Medicine
Guggenheim 18
Mayo Clinic
200 First Street SW
Rochester, MN 55905

E-mail: peng.kah@mayo.edu

Received for publication July 3, 2009;
accepted after revision November 12, 2009.

Published online: March 15, 2010.